

# Substrate specificity of SIRT1-catalyzed lysine N<sup>ε</sup>-deacetylation reaction probed with the side chain modified N<sup>ε</sup>-acetyl-lysine analogs

Nuttara Jamonnak<sup>1</sup>, Brett M. Hirsch, Yi Pang, Weiping Zheng\*

Department of Chemistry, University of Akron, 190 E. Buchtel Commons, Akron, OH 44325, USA

## ARTICLE INFO

### Article history:

Received 23 July 2009

Available online 24 October 2009

### Keywords:

N<sup>ε</sup>-acetyl-lysine

Analogs

SIRT1

Protein deacetylation

## ABSTRACT

Peptides containing L-N<sup>ε</sup>-acetyl-lysine (L-AcK) or its side chain modified analogs were prepared and assayed using SIRT1, the prototypical human silent information regulator 2 (Sir2) enzyme. While previous studies showed that the side chain acetyl group of L-AcK can be extended to bulkier acyl groups for Sir2 (including SIRT1)-catalyzed lysine N<sup>ε</sup>-deacetylation reaction, our current study suggested that SIRT1-catalyzed deacetylation reaction had a very stringent requirement for the distance between the α-carbon and the side chain acetamido group, with that found in L-AcK being optimal. Moreover, our current study showed that SIRT1 catalyzed the stereospecific deacetylation of L-AcK versus its D-isomer. The results from our current study shall constitute another piece of important information to be considered when designing inhibitors for SIRT1 and Sir2 enzymes in general.

© 2009 Elsevier Inc. All rights reserved.

## 1. Introduction

Silent information regulator 2 (Sir2) enzymes are a family of evolutionarily conserved proteins that are present in all kingdoms of life, with the yeast Sir2 being the founding member [1–3]. In humans, seven Sir2 orthologues, i.e. SIRT1–7, have been identified. Due to their well-conserved catalytic domains, Sir2 enzymes are all expected to catalyze the nicotinamide adenine dinucleotide (NAD<sup>+</sup>)-dependant deacetylation of L-N<sup>ε</sup>-acetyl-lysine (L-AcK) on protein substrates, with the formation of lysine N<sup>ε</sup>-deacetylated protein species and small molecule products, i.e. nicotinamide and 2'-O-acetyl-ADP-ribose which will be non-enzymatically equilibrated with 3'-O-acetyl-ADP-ribose in bulk solution (Fig. 1, R = CH<sub>3</sub>) [4–7]. Many acetylated protein substrates for the human Sir2 enzymes have been identified, such as the core histone proteins, various transcription factors, α-tubulin, acetyl-coenzyme A synthetase, and the Tat protein of human immunodeficiency virus type 1 (HIV-1). This deacetylation reaction has been shown to play a critical role in regulating multiple important biological processes such as transcriptional silencing, DNA repair, apoptosis, metabolism, aging, and HIV-1 infection [3,8–13]. As such, chemical modulation of the Sir2 deacetylase activity could offer therapeutic benefits for treating human diseases [3,14–22]. Indeed, genetic and pharmacological studies have suggested that human SIRT1 activation may alleviate type 2 diabetes, SIRT1 inhibition may be

an avenue for developing novel anti-cancer agents, and SIRT2 inhibition constitutes a novel therapeutic approach to Parkinson's disease.

During the past a few years, several classes of human Sir2 enzyme (especially SIRT1 and SIRT2) inhibitors have been identified [14,19,23,24], however, their inhibitory profiles (potency and selectivity) among all the human Sir2 enzymes are currently unknown. Moreover, the mechanism(s) of inhibition for the majority of currently identified human Sir2 inhibitors still awaits further elucidation. Therefore, developing novel inhibition strategies and inhibitors for the human Sir2 enzymes still constitutes a research area with tremendous current interest.

Even though a Sir2 enzyme is a deacetylase enzyme in that it can catalyze the removal of the side chain acetyl group of L-AcK (Fig. 1, R = CH<sub>3</sub>), a robust protein depropionylase activity to remove the side chain propionyl group of L-propionyl-lysine (Fig. 1, R = CH<sub>2</sub>CH<sub>3</sub>) and a robust protein debutyrylase activity to remove the side chain butyryl group of L-butyryl-lysine (Fig. 1, R = CH<sub>2</sub>CH<sub>2</sub>CH<sub>3</sub>) have also been recently reported for several Sir2 enzymes, including the human SIRT1 [25,26], the yeast Hst2 [26,27], and the bacterial enzymes Sir2Tm [28] and CobB [29]. This steric tolerance of a bulky acyl group has also been very recently manifested in the study by Asaba et al. [30] in which a stable potent and selective “bisubstrate-type” SIRT1 inhibitor was generated *in situ* from a L-AcK analog that bore an acyl group even bulkier than the butyryl group. While it is now known that the side chain acetyl group of L-AcK can be extended to bulkier acyl groups for Sir2-catalyzed lysine N<sup>ε</sup>-deacetylation reaction, in the current study, we were interested in examining whether the part of the side chain of L-AcK between the α-carbon and acetamide can tolerate structural perturbation for Sir2-catalyzed deacetylation

\* Corresponding author.

E-mail address: [wzheng@uakron.edu](mailto:wzheng@uakron.edu) (W. Zheng).

<sup>1</sup> Present address: Department of Molecular Biology and Genetics, Johns Hopkins University School of Medicine, 725 N. Wolfe Street, Baltimore, MD 21205, USA.

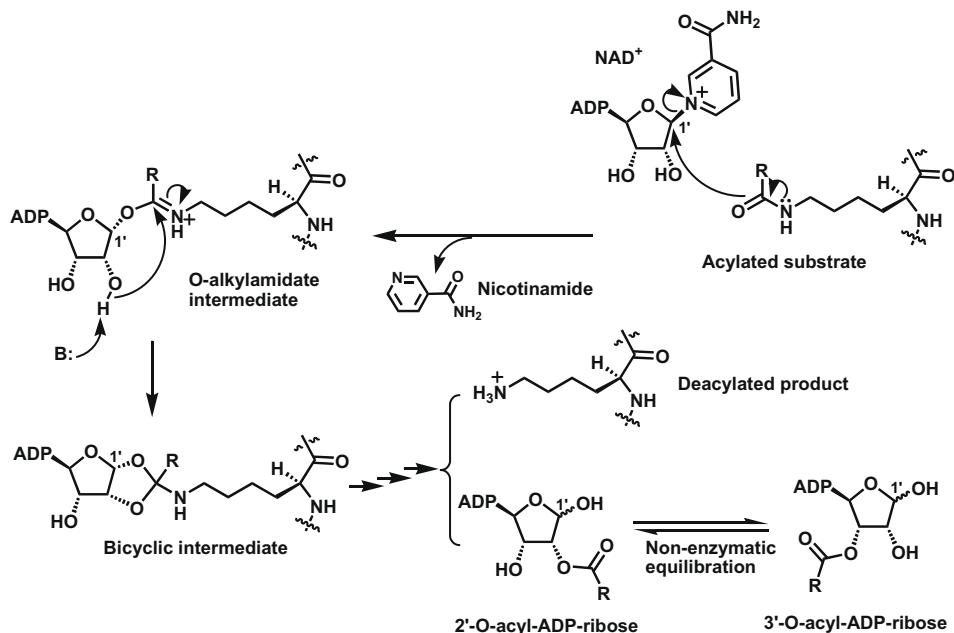


**Fig. 1.** The proposed chemical mechanism of the Sir2-catalyzed NAD<sup>+</sup>-dependent lysine N<sup>6</sup>-deacylation on protein substrates. The C1' position is indicated. ADP, adenosine diphosphate. R is CH<sub>3</sub>, CH<sub>2</sub>CH<sub>3</sub>, or CH<sub>2</sub>CH<sub>2</sub>CH<sub>3</sub>.

reaction. For this purpose, we prepared a series of the peptides that contained different L-AcK analogs with subtly different distances between the  $\alpha$ -carbon and the side chain acetamido group (Fig. 2). We showed that, as compared to the L-AcK-containing peptide, none of these peptides were able to be deacetylated under our experimental conditions by SIRT1, the model human enzyme that we chose for our study. These results suggested that the SIRT1-catalyzed deacetylation reaction had a very stringent requirement for the distance between the  $\alpha$ -carbon and the side chain acetamido group, with that found in L-AcK being optimal. The results from our current study shall constitute another piece of important information to be considered when designing Sir2 enzyme inhibitors.

## 2. Experimental

### 2.1. General

The following are the materials obtained from respective vendors for the synthesis of N<sup>α</sup>-Fmoc-protected amino acids and peptides used in the current study. All the materials were used as received without further purification. Sigma–Aldrich: DL-homocysteine, 1,4-

dioxane, silica gel (70–230 mesh, 60 Å), N-methylmorpholine (NMM), piperidine, phenol, thioanisole, ethanedithiol; Alfa Aesar: acetamidomethanol; Acros: L-homoserine; EMD biosciences: dichloromethane, trifluoroacetic acid (TFA), N,N-dimethylformamide (DMF), acetonitrile; Bachem: D-AcK; Novabiochem: all N<sup>α</sup>-Fmoc-protected amino acids except the analogs of L-N<sup>α</sup>-Fmoc-AcK that were synthesized in the current study, resins for the solid phase peptide synthesis (SPPS), 2-(1H-benzotriazole-1-yl)-1,1,3,3-tetramethylammonium hexafluorophosphate (HBTU, the coupling reagent used for SPPS), N-hydroxybenzotriazole (HOBT, the additive used for SPPS), N-(9-fluorenylmethyloxy-carbonyloxy)succinimide (Fmoc-OSu); Fisher: sodium carbonate, anhydrous diethyl ether.

<sup>1</sup>H and <sup>13</sup>C NMR spectra were obtained on a Varian Mercury 300 spectrometer or a Varian GEMINI 300 spectrometer. Mass spectra were recorded on a Bruker Reflex-III MALDI-TOF mass spectrometer or a Bruker Esquire-LC ion trap mass spectrometer (with electrospray ionization). High resolution mass spectra (HRMS) were obtained on a VG ZAB high resolution mass spectrometer at the high resolution mass spectrometry facility of the University of California, Riverside.

The following are the materials obtained for the expression and purification of GST-SIRT1 and the SIRT1 assays used in the current

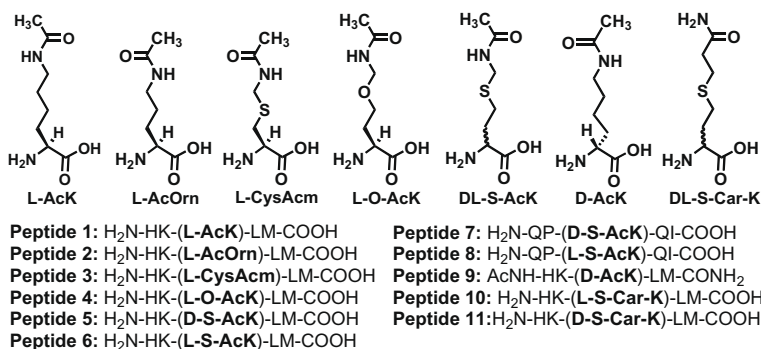


**Fig. 2.** L-AcK and its side chain modified analogs, and the corresponding peptides used in the current study. Peptides 5 and 7 were arbitrarily assigned to harbor D-S-AcK, and peptides 6 and 8 were arbitrarily assigned to harbor L-S-AcK. Peptide 10 was arbitrarily assigned to harbor L-S-Car-K, and peptide 11 was arbitrarily assigned to harbor D-S-Car-K. Ac, acetyl.

study: Plasmid pGEX2TK-P-SIRT1 (human full length) was a kind gift from Prof. Tony Kouzarides. *Escherichia coli* strain BL21(DE3) was purchased from Stratagene. Tryptone, yeast extract, isopropyl-1-thio- $\beta$ -D-galacto-pyranoside (IPTG), ampicillin, NaCl, KCl, and  $\text{NaH}_2\text{PO}_4$  were purchased from Fisher. Bacto Agar was purchased from BD Biosciences. Glycerol was from Acros. DL-dithiothreitol (DTT) was from EMD biosciences. Glutathione-agarose, L-glutathione reduced, trizma,  $\beta$ -NAD<sup>+</sup>, nicotinamide, guanidinium chloride, and a 1.0 M solution of  $\text{MgCl}_2$  (molecular-biology grade) were purchased from Sigma. All the materials obtained from commercial sources were used as received without further purification.

## 2.2. Molecular modeling

The HyperChem<sup>®</sup> 8.0 molecular modeling software was used to build and optimize the molecular geometry of L-AcK and each of its L-analogs with the Austin Model 1 (AM1) setting. The atom-to-atom distance was directly measured from the optimized structure. The HOMOs were also generated from the optimized molecular structures.

## 2.3. Synthesis of DL-N<sup>z</sup>-Fmoc-S-AcK

(a) To a stirred solution of DL-homocysteine (135 mg, 1 mmol) in TFA (4.5 mL) was added in three portions (at 0, 15, and 30 min) of acetamidomethanol (3  $\times$  30 mg, 1 mmol) at room temperature. After the third portion was added, the reaction mixture was stirred at room temperature for another 15 min before TFA was removed under reduced pressure. (b) To the resulting oily residue was added double deionized water (ddH<sub>2</sub>O) (5 mL), and the acidic solution was neutralized at 0 °C while stirring with a 10% (w/v) aqueous Na<sub>2</sub>CO<sub>3</sub> solution. Another portion of the 10% (w/v) Na<sub>2</sub>CO<sub>3</sub> solution (5 mL) was further added, and to the resulting solution was added dropwise a solution of Fmoc-OSu (675 mg, 2 mmol) in 1,4-dioxane (5 mL) at room temperature. After the addition was complete, the reaction mixture was stirred at room temperature for 5 h before ddH<sub>2</sub>O (50 mL) was added. The excess Fmoc-OSu was extracted away with diethyl ether (2  $\times$  100 mL). The aqueous layer was acidified with a 6.0 M aqueous HCl solution to pH  $\sim$  1 at 0 °C before being extracted with ethyl acetate (3  $\times$  100 mL). The organics were combined, dried with anhydrous Na<sub>2</sub>SO<sub>4</sub>, filtered, and concentrated under reduced pressure, affording a white solid residue from which the desired product was isolated *via* silica gel column chromatography as a white solid (270 mg, 63% after two steps): <sup>1</sup>H NMR (300 MHz, CDCl<sub>3</sub>):  $\delta$  (ppm) 7.78–7.19 (m, 8H, H<sub>arom</sub>), 4.38–4.02 (m, 6H, Fluorenyl H<sub>9</sub>, CH<sub>2</sub>O, CH<sub>2</sub>N and H<sub>alpha</sub>), 2.54–1.99 (m, 4H, CH<sub>2</sub>CH<sub>2</sub>), 1.91 (s, 3H, CH<sub>3</sub>); <sup>13</sup>C NMR (75 MHz, CDCl<sub>3</sub>):  $\delta$  (ppm) 175.1 (COOH), 173.2 (C(=O)NH), 156.9 (NHC(=O)O), 143.6 (C<sub>arom</sub>), 141.5 (C<sub>arom</sub>), 128.0 (C<sub>arom</sub>), 127.3 (C<sub>arom</sub>), 125.2 (C<sub>arom</sub>), 120.3 (C<sub>arom</sub>), 67.5 (CH<sub>2</sub>O), 60.1 (C<sub>alpha</sub>), 47.1 (Fluorenyl C<sub>9</sub>), 41.4 (CH<sub>2</sub>NH), 32.5 (CH<sub>2</sub>), 27.4 (CH<sub>2</sub>), 22.6 (CH<sub>3</sub>); HRMS (FAB) calcd. for C<sub>22</sub>H<sub>25</sub>N<sub>2</sub>O<sub>5</sub>S ([M + H]<sup>+</sup>) 429.1484; found: 429.1481.

## 2.4. Synthesis of DL-N<sup>z</sup>-Fmoc-S-Car-K

(a) To a stirred solution of 3-bromopropionamide (152 mg, 1 mmol) in freshly degassed methanol (33 mL) was added dropwise at room temperature a solution of DL-homocysteine (135 mg, 1 mmol) in a 1.0 M aqueous buffer solution of triethylammonium bicarbonate (pH 8.1–8.5) (33 mL). After the addition was complete, the reaction mixture was stirred at room temperature overnight under nitrogen before methanol was removed under reduced pressure. To the resulting residue was added ethyl acetate (60 mL) to extract away the unreacted 3-bromopropionamide. The aqueous phase was then lyophilized overnight, affording a white solid residue. (b) To the above-obtained white solid residue was added while stirring ddH<sub>2</sub>O

(5 mL) and a 10% (w/v) aqueous Na<sub>2</sub>CO<sub>3</sub> solution (5 mL). To the resulting stirred solution was added dropwise a solution of Fmoc-OSu (675 mg, 2 mmol) in 1,4-dioxane (5 mL) at room temperature. After the addition was complete, the reaction mixture was stirred at room temperature for 5 h before ddH<sub>2</sub>O (50 mL) was added. The excess Fmoc-OSu was extracted away with diethyl ether (2  $\times$  100 mL). The aqueous layer was acidified with a 6.0 M aqueous HCl solution to pH  $\sim$  1 at 0 °C before being extracted with ethyl acetate (3  $\times$  100 mL). The organics were combined, dried with anhydrous Na<sub>2</sub>SO<sub>4</sub>, filtered, and concentrated under reduced pressure, affording a white solid residue from which the desired product was isolated by reversed-phase high pressure liquid chromatography (HPLC) on a preparative C18 column (100 Å, 2.14  $\times$  25 cm). The HPLC column was eluted with a gradient of ddH<sub>2</sub>O containing 0.05% (v/v) of TFA and acetonitrile containing 0.05% (v/v) of TFA. The pooled HPLC fractions were stripped of acetonitrile and lyophilized to afford the desired product as a white solid (260 mg, 61% after two steps): <sup>1</sup>H NMR (300 MHz, CDCl<sub>3</sub>):  $\delta$  (ppm) 7.78–7.23 (m, 8H, H<sub>arom</sub>), 4.54–4.22 (m, 4H, Fluorenyl H<sub>9</sub>, CH<sub>2</sub>O, and H<sub>alpha</sub>), 2.82–2.09 (m, 8H, CH<sub>2</sub>CH<sub>2</sub>-S-CH<sub>2</sub>CH<sub>2</sub>); <sup>13</sup>C NMR (75 MHz, CD<sub>3</sub>OD):  $\delta$  (ppm) 174.4 (COOH), 174.1 (C(=O)NH<sub>2</sub>), 155.6 (NHC(=O)O), 143.9 (C<sub>arom</sub>), 141.4 (C<sub>arom</sub>), 127.6 (C<sub>arom</sub>), 127.0 (C<sub>arom</sub>), 125.1 (C<sub>arom</sub>), 119.7 (C<sub>arom</sub>), 66.8 (CH<sub>2</sub>O), 53.0 (C<sub>alpha</sub>), 47.0 (Fluorenyl C<sub>9</sub>), 35.6 (CH<sub>2</sub>), 31.5 (CH<sub>2</sub>), 28.0 (CH<sub>2</sub>), 27.0 (CH<sub>2</sub>); HRMS (FAB) calcd. for C<sub>22</sub>H<sub>25</sub>N<sub>2</sub>O<sub>5</sub>S ([M + H]<sup>+</sup>) 429.1471; found: 429.1468.

## 2.5. Synthesis of L-N<sup>z</sup>-Fmoc-O-AcK

Essentially the same synthetic procedure as that described above for the synthesis of DL-N<sup>z</sup>-Fmoc-S-AcK was followed except that L-homoserine (119 mg, 1 mmol) was used instead of DL-homocysteine. After two steps of reactions (Scheme 2), the desired product was isolated *via* silica gel column chromatography as a white solid (180 mg, 44% after two steps): <sup>1</sup>H NMR (300 MHz, CDCl<sub>3</sub>):  $\delta$  (ppm) 7.44–6.98 (m, 8H, H<sub>arom</sub>), 4.31–3.88 (m, 6H, Fluorenyl H<sub>9</sub>, CH<sub>2</sub>O, OCH<sub>2</sub>N and H<sub>alpha</sub>), 3.27–1.74 (m, 4H, CH<sub>2</sub>CH<sub>2</sub>), 1.69 (s, 3H, CH<sub>3</sub>); <sup>13</sup>C NMR (75 MHz, CDCl<sub>3</sub>):  $\delta$  (ppm) 175.2 (COOH), 173.0 (C(=O)NH), 156.7 (NHC(=O)O), 143.8 (C<sub>arom</sub>), 141.4 (C<sub>arom</sub>), 128.0 (C<sub>arom</sub>), 127.3 (C<sub>arom</sub>), 125.3 (C<sub>arom</sub>), 120.2 (C<sub>arom</sub>), 70.4 (OCH<sub>2</sub>NH), 67.3 (CH<sub>2</sub>O), 64.7 (side chain CH<sub>2</sub>O), 58.7 (C<sub>alpha</sub>), 47.2 (Fluorenyl C<sub>9</sub>), 31.7 (CH<sub>2</sub>), 25.5 (CH<sub>3</sub>); HRMS (FAB) calcd. for C<sub>22</sub>H<sub>25</sub>N<sub>2</sub>O<sub>6</sub> ([M + H]<sup>+</sup>) 413.1713; found: 413.1710.

## 2.6. Synthesis of D-N<sup>z</sup>-Fmoc-AcK

To a stirred solution of D-AcK (188 mg, 1 mmol) in aqueous 10% (w/v) Na<sub>2</sub>CO<sub>3</sub> (10 mL) was added dropwise a solution of Fmoc-OSu (675 mg, 2 mmol) in 1,4-dioxane (5 mL) at room temperature. After the addition was complete, the reaction mixture was stirred at room temperature for 5 h before ddH<sub>2</sub>O (50 mL) was added. The excess Fmoc-OSu was extracted away with diethyl ether (2  $\times$  100 mL). The aqueous layer was acidified with a 6.0 M aqueous HCl solution to pH  $\sim$  1 at 0 °C before being extracted with ethyl acetate (3  $\times$  100 mL). The organics were combined, dried with anhydrous Na<sub>2</sub>SO<sub>4</sub>, filtered, and concentrated under reduced pressure, affording an oily residue from which the desired product was isolated *via* silica gel column chromatography as a white solid (231 mg, 56%): <sup>1</sup>H NMR (300 MHz, CD<sub>3</sub>OD):  $\delta$  (ppm) 7.79–7.26 (m, 8H, H<sub>arom</sub>), 4.34–4.07 (m, 4H, Fluorenyl H<sub>9</sub>, CH<sub>2</sub>O, and H<sub>alpha</sub>), 3.14 (t, J = 6.6 Hz, 2H, CH<sub>2</sub>N), 1.89 (s, 3H, CH<sub>3</sub>), 1.89–1.32 (m, 6H, CH<sub>2</sub>CH<sub>2</sub>CH<sub>2</sub>); <sup>13</sup>C NMR (75 MHz, CDCl<sub>3</sub>):  $\delta$  (ppm) 172.5 (COOH), 164.2 (C(=O)NH), 158.0 (NHC(=O)O), 144.5 (C<sub>arom</sub>), 141.9 (C<sub>arom</sub>), 128.1 (C<sub>arom</sub>), 127.5 (C<sub>arom</sub>), 125.6 (C<sub>arom</sub>), 120.2 (C<sub>arom</sub>), 67.2 (CH<sub>2</sub>O), 54.9 (C<sub>alpha</sub>), 47.4 (Fluorenyl C<sub>9</sub>), 39.6 (CH<sub>2</sub>N), 29.2 (CH<sub>2</sub>), 25.6 (CH<sub>2</sub>), 23.6 (CH<sub>2</sub>), 21.8 (CH<sub>3</sub>); MS (ESI): *m/z* 411 [M + H]<sup>+</sup>, 433 [M + Na]<sup>+</sup>. HRMS (FAB) calcd. for C<sub>23</sub>H<sub>25</sub>N<sub>2</sub>O<sub>5</sub> ([M – H]<sup>–</sup>) 409.1758; found: 409.1759.

## 2.7. Peptide synthesis and purification

All peptides were synthesized using the Fmoc chemistry-based SPPS [31] on a PS3 peptide synthesizer (Protein Technologies Inc., Tucson, AZ, USA). One to two equivalents of the analogs of L-N<sup>α</sup>-Fmoc-AcK that were synthesized in the current study (i.e. DL-N<sup>α</sup>-Fmoc-S-AcK, DL-N<sup>α</sup>-Fmoc-S-Car-K, L-N<sup>α</sup>-Fmoc-O-AcK, and D-N<sup>α</sup>-Fmoc-AcK) were used in 9-h coupling reactions to incorporate the respective L-AcK analogs into peptides. However, for all other N<sup>α</sup>-Fmoc-protected amino acids, four equivalents were used in 1-h coupling reactions. All the peptides were cleaved from the resin by reagent K (83.6% (v/v) TFA, 5.9% (v/v) phenol, 4.2% (v/v) ddH<sub>2</sub>O, 4.2% (v/v) thioanisole, 2.1% (v/v) ethanedithiol), precipitated in cold diethyl ether, and purified by reversed-phase HPLC on a preparative C18 column (100 Å, 2.14 × 25 cm). The HPLC column was eluted with a gradient of ddH<sub>2</sub>O containing 0.05% (v/v) of TFA and acetonitrile containing 0.05% (v/v) of TFA. The pooled HPLC fractions were stripped of acetonitrile and lyophilized to give all peptides as puffy white solids. Peptide purity (>95%) was verified by reversed-phase HPLC on an analytical column (100 Å, 0.46 × 25 cm), and their molecular weights were confirmed by either matrix assisted laser desorption ionization-time of flight (MALDI-TOF) or electrospray ionization (ESI) mass spectrometric analysis.

## 2.8. Expression and purification of GST-SIRT1

The following procedure was derived with modifications from those described previously [32–34]. Following the transformation of pGEX2TK-P · SIRT1 (human full length) into the *Escherichia coli* strain BL21(DE3), one of the resulting colonies was used to inoculate a 10-mL Luria Broth containing 100 µg/mL of ampicillin, and the culture was grown at 37 °C overnight (18 h). This culture was subsequently used to inoculate a 1-L Luria Broth also containing 100 µg/mL of ampicillin, and the culture was grown at 37 °C until the optical density (OD) at 600 nm reached 0.6. Fresh 1.0 M IPTG was then added to the culture to a final concentration of 0.3 mM, and the culture was grown at 16 °C for an additional 20 h. The cells were harvested by centrifugation at 3500 rpm and 4 °C for 20 min, and the pellet was resuspended in 25 mL of the ice-cold lysis buffer (25 mM sodium phosphate buffer (pH 7.4), 130 mM NaCl, 5 mM DTT, 10% (v/v) glycerol, and 1 mM phenylmethylsulphonyl fluoride (PMSF)). Resuspended cells were lysed by double passage through a French pressure cell at 700 psi and centrifuged at 15,000 rpm and 4 °C for 30 min to remove cell debris. The supernatant was loaded onto a plastic column packed with 350 mg of the glutathione-agarose that had been pre-swollen in 30 mL of ddH<sub>2</sub>O and equilibrated with 50 mL of the ice-cold lysis buffer without PMSF. The glutathione-agarose beads were then washed with 40 mL of a high salt buffer (25 mM sodium phosphate buffer (pH 7.4), 387 mM NaCl, 5 mM DTT, 10% (v/v) glycerol). The GST-SIRT1 protein was eluted off of the column with the elution buffer (25 mM sodium phosphate buffer (pH 7.4), 241 mM NaCl, 5 mM DTT, 50 mM L-glutathione reduced, 10% (v/v) glycerol). The pooled fractions (~10 mL) were dialyzed against the storage buffer (25 mM Tris-HCl (pH 7.5), 100 mM NaCl, 5 mM DTT, 10% (v/v) glycerol), aliquoted, snap frozen with liquid N<sub>2</sub>, and stored at –80 °C. The protein concentration (1.5 mg/mL) was determined by the Bradford assay.

## 2.9. HPLC-based SIRT1 time-course assay

A SIRT1 time-course assay solution contained the following components: 25 mM Tris-HCl (pH 8.0), 137 mM NaCl, 2.7 mM KCl, 1 mM MgCl<sub>2</sub>, 0.5 mM β-NAD<sup>+</sup>, 350 nM GST-SIRT1, and 0.3 mM of a pentapeptide (i.e. peptides **1–11**). An enzymatic reaction was initiated by the addition of GST-SIRT1 at 37 °C and was

incubated at 37 °C until quenched at different time points (0, 30, 60, and 120 min) with the following stop solution: 3.2 M guanidinium chloride in 0.1 M of sodium phosphate buffer (pH 6.8). One portion (40 µL) of the SIRT1 assay mixture was quenched with 80 µL of the above stop solution and was analyzed by reversed-phase HPLC with a C18 analytical column (100 Å, 0.46 × 25 cm). For assessing the possible SIRT1-catalyzed deacetylation, the C18 analytical column was eluted with the following gradient of ddH<sub>2</sub>O containing 0.05% (v/v) TFA (mobile phase A) and acetonitrile containing 0.05% (v/v) TFA (mobile phase B): linear increase from 0% B to 50% B from 0 to 40 min (1 mL/min), and ultraviolet (UV) monitoring at 214 nm. For assessing the possible SIRT1-catalyzed nicotinamide production, the C18 analytical column was eluted with the following gradient of mobile phase A and mobile phase B: linear increase from 0% B to 15% B from 0 to 40 min (1 mL/min), and monitored with UV at 261 nm.

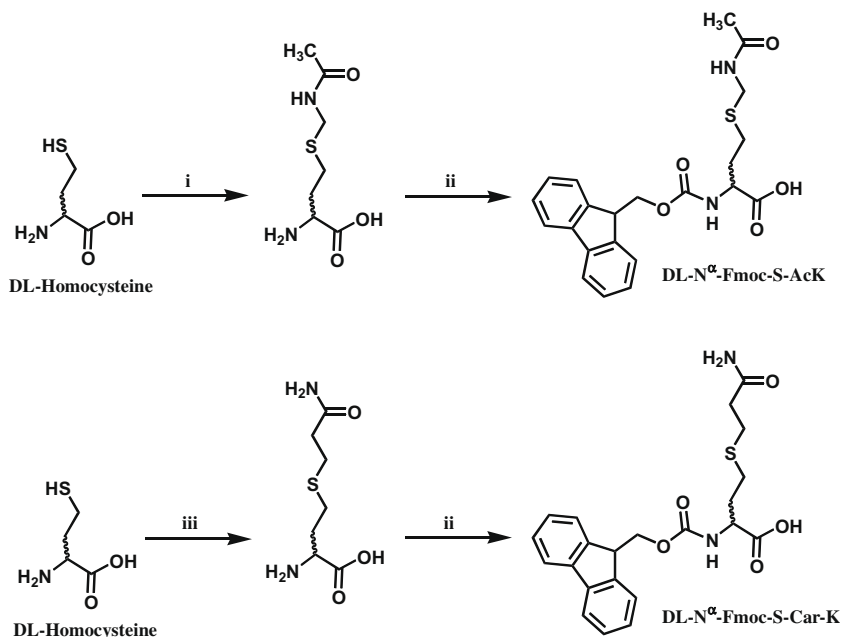
## 2.10. HPLC-based SIRT1 inhibition assay

A SIRT1 inhibition assay solution (100 µL) contained the following components: 25 mM Tris-HCl (pH 8.0), 137 mM NaCl, 2.7 mM KCl, 1 mM MgCl<sub>2</sub>, 0.5 mM β-NAD<sup>+</sup>, 0.1 mM peptide **1**, 350 nM GST-SIRT1, and a pentapeptide (peptides **5**, **6**, **10**, or **11**) varied from 0 to 1.6 mM. An enzymatic reaction was initiated by the addition of GST-SIRT1 at 37 °C and was incubated at 37 °C for 10 min before quenched with 25 µL of a stop solution composed of 0.1 M HCl and 0.16 M acetic acid. The enzymatic deacetylation product (i.e. peptide **1a** in Fig. 5) was detected and quantified by reversed-phase HPLC with a C18 analytical column (100 Å, 0.46 × 25 cm), eluting with the following gradient of ddH<sub>2</sub>O containing 0.05% (v/v) TFA (mobile phase A) and acetonitrile containing 0.05% (v/v) TFA (mobile phase B): linear increase from 0% B to 50% B from 0 to 40 min (1 mL/min), and UV monitoring at 214 nm.

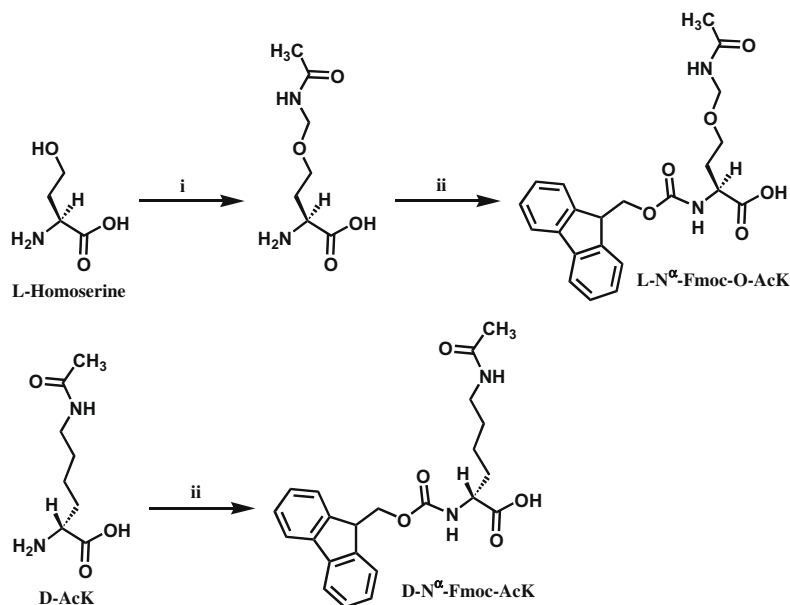
## 3. Results and discussion

### 3.1. Synthesis of the side chain modified L-AcK analogs and the corresponding peptides

All the peptides used in the current study were synthesized using the Fmoc chemistry-based SPPS [31] (see Section 2). In order to incorporate L-AcK and its analogs into peptides, their corresponding N<sup>α</sup>-Fmoc-protected derivatives were either obtained from commercial sources if available or synthesized as described below. L-N<sup>α</sup>-Fmoc-AcK, L-N<sup>α</sup>-Fmoc-AcOrn, and L-N<sup>α</sup>-Fmoc-CysAcM that were used to incorporate respectively L-AcK, L-AcOrn, and L-CysAcM into peptides **1**, **2**, and **3** were commercially available. Scheme 1 depicts the synthesis of DL-N<sup>α</sup>-Fmoc-S-AcK and DL-N<sup>α</sup>-Fmoc-S-Car-K. Of note, DL-N<sup>α</sup>-Fmoc-S-AcK was synthesized using a modified literature procedure [35]. Even though L-homocysteine is also commercially available, we expected that racemization of this starting material and the product might occur under the given reaction condition (room temperature, overnight, pH 8.1–8.5) during the first step of the synthesis of DL-N<sup>α</sup>-Fmoc-S-Car-K, therefore, we used the commercially available racemic starting material (i.e. DL-homocysteine) for the synthesis. DL-homocysteine was also used to synthesize DL-N<sup>α</sup>-Fmoc-S-AcK. However, even though DL-N<sup>α</sup>-Fmoc-S-AcK and DL-N<sup>α</sup>-Fmoc-S-Car-K were obtained in our synthesis, following their use to incorporate DL-S-AcK and DL-S-Car-K into peptides, we were able to, in each case, separate the two diastereomeric peptides harboring either the D- or the L-enantiomer of an analog with HPLC, affording peptides **5–8**, **10**, and **11**. Scheme 2 depicts the synthesis of L-N<sup>α</sup>-Fmoc-O-AcK and D-N<sup>α</sup>-Fmoc-AcK that were used to incorporate respectively



**Scheme 1.** Reagents: (i) acetamidomethanol, TFA. (ii) Fmoc-OSu, 1,4-dioxane, 10% (w/v) aq. Na<sub>2</sub>CO<sub>3</sub>. (iii) 3-Bromopropionamide, degassed MeOH, 1.0 M Et<sub>3</sub>NH<sup>+</sup> · HCO<sub>3</sub><sup>-</sup> (pH 8.1–8.5).



**Scheme 2.** Reagents: (i) acetamidomethanol, TFA. (ii) Fmoc-OSu, 1,4-dioxane, 10% (w/v) aq. Na<sub>2</sub>CO<sub>3</sub>.

L-O-AcK and D-AcK into peptides **4** and **9**. It should be noted that the S-acetamidomethyl (S-Acm)-containing side chains of L-Cy-sAcm and D-(or L)-S-AcK as well as the O-acetamidomethyl (O-Acm)-containing side chain of L-O-AcK were observed to be chemically stable enough to survive our experimental conditions for the peptide synthesis and purification, as well as the SIRT1 assays. This chemical stability is consistent with the fact that Acm can be used as an acid/base stable thiol protecting group (e.g. for cysteine) during SPPS [36] and with the literature report of the peptides containing the O-Acm group on serine and threonine side chains, as well as the acid/base stable serine analog whose side chain contained O-Acm [37].

### 3.2. Design of the side chain modified L-AcK analogs and the corresponding peptides

#### 3.2.1. Peptide sequence selection

Fig. 2 shows the structures of L-AcK and its side chain modified analogs, as well as the corresponding peptides used in the current study. Peptides **1–6** and **9–11** were constructed based on the sequence (amino acid residue 380–384) derived from the C-terminal region of the human p53 protein [38]. Since the 382 position was shown to be the *in vivo* SIRT1 deacetylation site of the human p53 protein [39], L-AcK or its analogs were thus each incorporated into this position in a peptide. Furthermore, the 5-residue peptide

(i.e. peptide **1**) was shown by Garske et al. [40] and our current study to serve as a good SIRT1 substrate, therefore, we also used this 5-residue sequence to construct peptides **2–6** and **9–11**. Since Garske et al. also reported previously that H<sub>2</sub>N-QP-(L-AcK)-QI-COOH was a ~9-fold better SIRT1 substrate than H<sub>2</sub>N-HK-(L-AcK)-LM-COOH, as judged by  $k_{cat}/K_m$  ratios [40], peptides **7** and **8** were also prepared in the current study to examine whether the use of a better SIRT1 peptide substrate sequence could have an effect on SIRT1 processing of a given L-AcK analog.

### 3.2.2. Design of L-AcK analogs

**3.2.2.1. L-Analogs with varied side chain carbonyl oxygen- $\alpha$  carbon distances.** As described in Section 3.3, deleting one methylene group from the side chain of L-AcK seemed to be a too drastic side chain length perturbation for the SIRT1-catalyzed deacetylation reaction to take place, since the SIRT1-catalyzed deacetylation was not observed for the peptide containing L-acetyl-ornithine (L-AcOrn) (i.e. peptide **2**, Fig. 2) under our experimental conditions, which is in stark contrast to a robust SIRT1-catalyzed deacetylation of the L-AcK-containing peptide (i.e. peptide **1**, Fig. 2). Therefore, we were interested in coming up with further L-AcK analogs whose distances between the  $\alpha$ -carbon and the side chain acetamide will be between that in L-AcOrn and that in L-AcK. In addition, we were also interested in evaluating those side chains that are longer than that of L-AcK but less than lengthening by one methylene group.

To help guide our design of such analogs, we used the HyperChem<sup>®</sup> software to optimize the molecular geometry of L-AcK and its analogs and then to compare the distance between the  $\alpha$ -carbon and the side chain carbonyl oxygen atom from each geometrically optimized structure. Of note, we used this distance as the parameter of comparison because the side chain carbonyl oxygen atom of L-AcK serves as a nucleophile to attack the C1' atom of NAD<sup>+</sup> during the first chemical step of Sir2 enzymatic catalysis (Fig. 1). Fig. 3 shows the optimized geometry of L-AcK and its L-analogs, as well as the distance between the  $\alpha$ -carbon and the side chain carbonyl oxygen atom from each geometrically optimized structure. From shortest to longest, these distances are: L-AcOrn, 6.62 Å; L-CysAcm, 6.80 Å; L-O-AcK, 7.47 Å; L-AcK, 7.64 Å; L-S-Car-K, 7.78 Å; L-S-AcK, 8.00 Å. Since one methylene group is worth of 1.02 Å which is the difference between the distances in L-AcK and L-AcOrn (i.e. 7.64–6.62 Å), the above distances form a finetuned spectrum within one methylene group deviation from the side chain of L-AcK. It is apparent from Fig. 3 that all of the geometrically optimized side chains assume the fully extended conformation, thus mimicking that of the side chain of L-AcK bound to its hydrophobic tunnel at a Sir2 enzyme active site [41,42]. In our opinion, this conformational mimicry makes the above distance comparison a reasonable reflection of the corresponding distance differences among the side chains if they are able to bind to the SIRT1 active site.

Among all the side chain structures shown in Fig. 3, only one is not terminated with the acetamido group, that is the side chain of L-S-Car-K that is terminated with a primary carboxamide. However, the distance between the  $\alpha$ -carbon and the side chain carbonyl oxygen atom of this analog (i.e. 7.78 Å) is the closest distance to that in L-AcK (7.64 Å) among all the distances shown in Fig. 3, and because of this, the peptide containing this analog (i.e. peptide **10**, Fig. 2) and the peptide containing its D-isomer (i.e. peptide **11**, Fig. 2) were also prepared (see Section 3.1) and assayed with SIRT1 (see Section 3.3). Even though the side chain of L-S-Car-K terminates with a primary carboxamide instead of an acetamide, the oxygen atom of the carboxamide is presumably able to function similarly to that of acetamide for the nucleophilic attack at the C1' atom of NAD<sup>+</sup> (Fig. 1) as long as the oxygen atom is positioned correctly relative to the C1' atom of NAD<sup>+</sup>.

All together, two L-analogs with longer distances and three L-analogs with shorter distances as shown in Fig. 3 were designed.

It should be noted that, in order to subtly change the length between the  $\alpha$ -carbon and the side chain acetamide of L-AcK, we used S and O atoms as the isosteric replacements for CH<sub>2</sub>. In the side chain of L-S-Car-K, we also made the isosteric swapping of the NH and CH<sub>3</sub> groups of the acetamide.

### 3.2.2.2. Predicted similar side chain carbonyl oxygen nucleophilicity in L-AcK and its L-analogs.

It should be noted that the introduction of the more electronegative heteroatoms S and O (than C) in the designed L-analogs may alter the nucleophilicity of the nearby carbonyl oxygen atom which, if positioned correctly, will serve as a nucleophile to attack the electrophilic C1' atom of NAD<sup>+</sup>, as shown in Fig. 1. However, when we calculated the highest occupied molecular orbitals (HOMOs) involving the side chain carbonyl oxygen atoms for L-AcK and its two heteroatom (O or S)-containing acetamide analogs (i.e. L-O-AcK and L-S-AcK), very similar orbital lobes were observed on the carbonyl oxygen atoms among these three structures (Fig. 4), suggesting that very similar nucleophilicity is expected when the carbonyl oxygen attacks the C1' atom of NAD<sup>+</sup>. In our opinion, the three HOMOs shown in Fig. 4 should be able to serve as the representatives for all the L-analogs shown in Fig. 3. Specifically, the HOMO of L-AcK will also represent those of L-S-Car-K and L-AcOrn, and the HOMO of L-S-AcK will also represent that of L-CysAcm. It is also noted from Fig. 4 that the lone pair electrons on the heteroatom near the center of the molecule tend to contribute to the HOMO through hyperconjugation with adjacent C–H bonds. Although this heteroatom impact is evident in the HOMO of L-O-AcK, its effect on the side chain carbonyl oxygen appears to be minimal (in terms of the orbital lobe size on the carbonyl oxygen). In the case of L-S-AcK, contribution to HOMO from the sulfur atom becomes negligible, partly attributing to the longer C–S bond which weakens the hyperconjugation with C–H bonds.

The above modeling results thus suggested that the side chain carbonyl oxygen atoms in L-AcK and its L-analogs (Fig. 3) are anti-

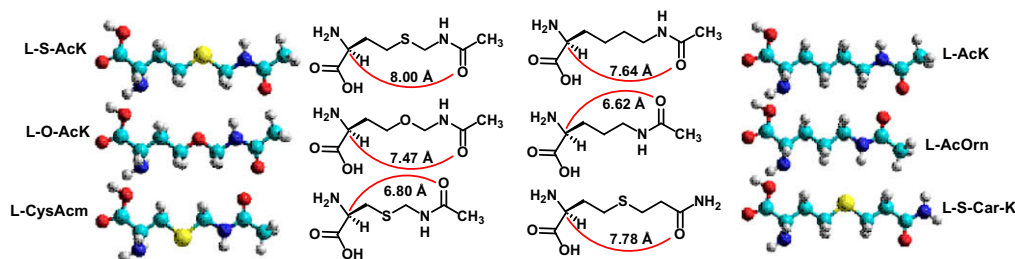


**Fig. 3.** Optimized molecular geometry of L-AcK and its L-analogs. Atomic color code: H, white; C, light blue; O, red; N, blue; S, yellow. The distances between the side chain carbonyl oxygen atom and the  $\alpha$ -carbon were indicated for L-AcK and each of the analogs. (For interpretation of the references to color in this figure legend, the reader is referred to the web version of this article.)

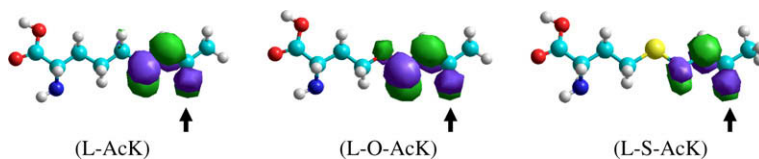


**Fig. 4.** Representative HOMOs involving the side chain carbonyl oxygen atoms (arrow indicated) for L-AcK (left), L-O-AcK (middle), and L-S-AcK (right).

ipated to exhibit very similar nucleophilicity while their relative positions to the  $\alpha$ -carbon atoms are varied.

**3.2.2.3. D-Analogs.** Besides the above-described L-analogs, three D-analogs of L-AcK were also involved in the current study. The peptide containing D-AcK (i.e. peptide **9**, Fig. 2) was used to directly examine whether SIRT1 can catalyze the stereospecific deacetylation of L-AcK versus its D-isomer. The remaining D-analog-containing peptides include peptides **5** and **7** both containing D-S-AcK and peptide **11** containing D-S-Car-K (Fig. 2). From the analog synthesis standpoint, these latter three D-analog-containing peptides were also produced (see Section 3.1), however, the additional evaluation of these peptides in SIRT1 assays nevertheless made a further contribution to our understanding of the molecular behavior of the L-AcK analogs used in the current study (see Section 3.3).

### 3.3. SIRT1 assays of peptides containing L-AcK or its analogs

We initially subjected the peptides shown in Fig. 2 that are terminated with the acetamido group (i.e. peptides **1–9**) to a HPLC-based SIRT1 deacetylation time-course assay [43–45]. When the positive control peptide (i.e. peptide **1**) was incubated with GST-SIRT1 at 37 °C for 1 h, around 20% of substrate deacetylation was already observed (Fig. 5). However, no enzymatic deacetylation peptide product was able to be detected for peptides **2–9** even after a 2-h incubation with GST-SIRT1 at 37 °C. Fig. 5 also shows the rep-

resentative HPLC chromatograms for the assay with peptide **6**, one of the test peptides. Since the reliable detection limit of our HPLC-based assay is  $\sim 1 \mu\text{M}$  and around 40% of substrate deacetylation was observed for peptide **1** after a 2-h incubation with GST-SIRT1 (HPLC assay chromatogram not shown), peptides **2–9** were thus each at least  $\sim 120$ -fold worse than peptide **1** toward deacetylation by SIRT1 under our experimental conditions.

The fact that same phenomena were observed for peptides **5** and **6** versus peptides **7** and **8** that contain the same pair of L-AcK analogs (i.e. D-S-AcK and L-S-AcK) argue that our observations in the current study resulted from the intrinsic properties of the side chains found in the analogs, because they do not depend on the peptide sequence context. Since a detectable enzymatic deacetylation was not observed from the D-AcK-containing peptide **9** under the same SIRT1 time-course assay condition under which the L-AcK-containing peptide **1** was shown to give rise to a robust deacetylation signal, SIRT1 can thus catalyze the stereospecific deacetylation of L-AcK versus its D-isomer.

Besides the above-described SIRT1 deacetylation assay to assess the possible enzymatic formation of a deacetylated peptide product, we also performed the HPLC-based time-dependent nicotinamide formation assay to assess the effect of the side chain structural deviation from L-AcK on SIRT1-catalyzed nicotinamide production from the L-AcK-containing peptide (i.e. the positive control peptide **1**), which is the first chemical step along the reaction coordinate of Sir2-catalyzed deacetylation reaction (Fig. 1). In

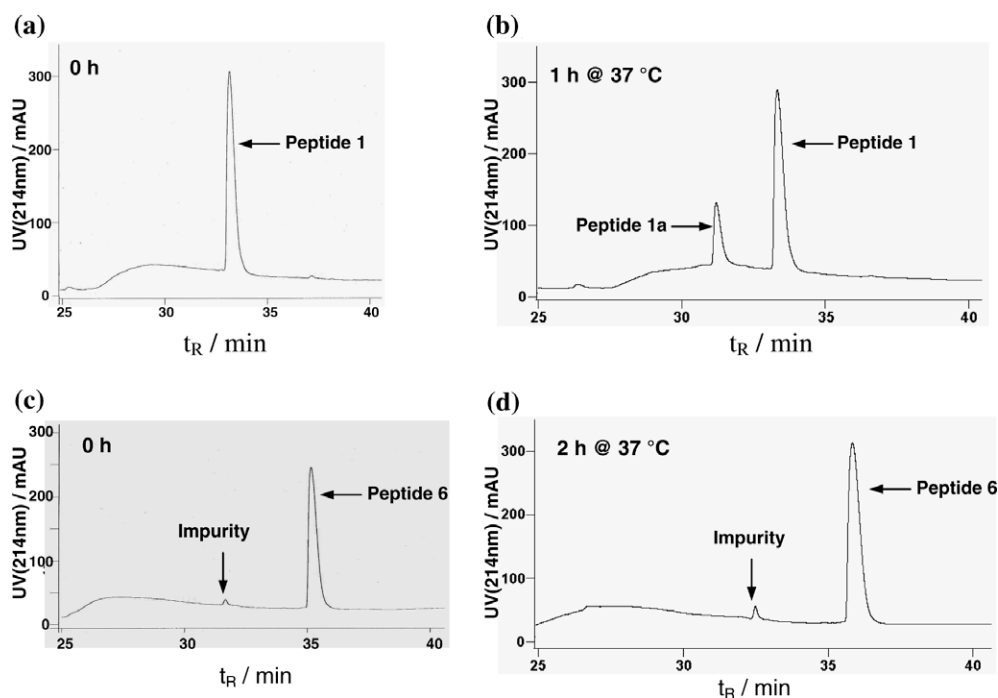


**Fig. 5.** Representative reversed-phase HPLC chromatograms from a SIRT1 time-course assay to assess the possible enzymatic formation of a deacetylated peptide product. Peptide **1a** ( $\text{H}_2\text{N-HKKLM-COOH}$ ; MS (MALDI-TOF):  $m/z$  656  $[\text{M} + \text{H}]^+$ , 678  $[\text{M} + \text{Na}]^+$ , 694  $[\text{M} + \text{K}]^+$ ) is the SIRT1-catalyzed deacetylation product from peptide **1** (also compare chromatograms (a) and (b)). All assays were performed in duplicate and essentially the same assay HPLC chromatograms were obtained for duplicates. The small peak with  $t_R \sim 32.5$  min in chromatogram (d) was from a minor impurity in the purified peptide **6** sample (as shown in chromatogram (c)), rather than the deacetylated product.

specific, we assayed peptide **1** and peptides **2–6** and **9–11** that each contains a unique analog of L-AcK (Fig. 2). In consistent with the observed robust SIRT1-catalyzed deacetylation of peptide **1**, a robust SIRT1-catalyzed nicotinamide production from peptide **1** was also observed in that around 8.9% of NAD<sup>+</sup> cleavage (to form nicotinamide) was already observed following the incubation of peptide **1** with GST-SIRT1 at 37 °C for 30 min. However, no enzymatic nicotinamide formation was detected from peptides **2–6** and **9–11** even after a 2-h incubation with GST-SIRT1 at 37 °C.

While further studies are needed to unambiguously account for the above-described lack of observable enzymatic deacetylation and/or nicotinamide formation from peptides containing L-AcK analogs, our current hypothesis is that the side chain of a D-analog is unable to bind to the L-AcK binding tunnel at the SIRT1 active site, whereas the side chain of a L-analog is able to bind to the L-AcK binding tunnel, but with the side chain carbonyl oxygen atom being positioned incorrectly relative to the C1' atom of NAD<sup>+</sup>. Of note, as described in Section 3.2, the nucleophilicity of the side chain carbonyl oxygen atoms in L-AcK and its analogs was predicted to be similar based on the calculated HOMOs. As a support to our hypothesis, the side chains of several L-analogs of L-AcK, including L-thioacetyl-lysine and those with acyl groups bulkier than the acetyl group, were previously shown to be able to be accommodated at the active sites of SIRT1 and several other Sir2 enzymes when placed within different peptide contexts [25–29,43,44,46].

To preliminarily address our hypothesis, we first turned our attention to the pair of the peptides (i.e. peptides **10** and **11**, Fig. 2) that respectively contain L-S-Car-K and D-S-Car-K, since the distance between the  $\alpha$ -carbon and the carbonyl oxygen atom in this side chain (7.78 Å) is the closest one to that in L-AcK (7.64 Å) among all the distances shown in Fig. 3. When these two peptides were examined for their respective inhibitory potency against SIRT1-catalyzed deacetylation of peptide **1**, we found that, while peptide **11** did not exhibit any inhibition at 1.6 mM, 81% inhibition was observed for peptide **10** at 1.6 mM. Since the only difference between peptides **10/11** and peptide **1** is their containing different side chains at the central position, the different inhibitory potency that we observed for peptides **10** and **11** shall also reflect the different potency of these two peptides to compete with the binding of peptide **1** at SIRT1 active site. Therefore, this SIRT1 inhibition experimental result strongly suggested that the side chain of D-S-Car-K was unable to bind to the L-AcK binding tunnel at the SIRT1 active site, whereas the side chain of L-S-Car-K was able to, but with the side chain carbonyl oxygen atom being positioned incorrectly relative to the C1' atom of NAD<sup>+</sup>, which could account for our inability to detect the enzymatic nicotinamide formation from both peptides **10** and **11**. Within this context, the incorrect side chain carbonyl oxygen positioning relative to the C1' atom of NAD<sup>+</sup> within the L-AcK binding tunnel could also account for our inability to observe the enzymatic deacetylation and nicotinamide formation from peptide **4** which contains L-O-AcK, another L-AcK analog that also has a fairly close distance between the  $\alpha$ -carbon and the side chain carbonyl oxygen to that in L-AcK (i.e. 7.47 Å versus 7.64 Å, Fig. 3).

To extend the above-described pairwise analysis with peptides **10** and **11**, we next examined the SIRT1 inhibitory potency of peptides **5** and **6**, one of the two pairs of the peptides that respectively contain D-S-AcK and L-S-AcK (Fig. 2). It turned out that peptide **5** did not exhibit any inhibition at 1.6 mM, whereas 14% inhibition was observed for peptide **6** at 1.6 mM. The differential extents of SIRT1 inhibition exhibited by peptides **5** and **6** also strongly suggested that the side chain of D-S-AcK was unable to bind to the L-AcK binding tunnel, whereas the side chain of L-S-AcK was able to. Our inability to observe the enzymatic deacetylation and nicotinamide formation from peptide **6** could also be explained by the

incorrect positioning of its side chain carbonyl oxygen relative to the C1' atom of NAD<sup>+</sup> within the L-AcK binding tunnel.

The above-described two pairwise SIRT1 inhibition experiments not only furnished evidence in favor of our hypothesis, but also suggested that peptide **6** has a weaker binding affinity than peptide **10**, even though both seemed to bind weakly as compared to peptide **1**, considering that we used 100  $\mu$ M of peptide **1** in the inhibition assay. This could be due to the suboptimal positioning of the side chains of both L-S-Car-K and L-S-AcK within the L-AcK binding tunnel as compared to the side chain of L-AcK, however, that of L-S-AcK is the least optimal side chain among the three. This latter notion is consistent with the greater deviation of the distance between the  $\alpha$ -carbon and the side chain carbonyl oxygen from that of L-AcK for L-S-AcK than L-S-Car-K (Fig. 3). The SIRT1 inhibition results with peptides **10** and **6** further suggested that the L-AcK binding tunnel could also accommodate an atom/group (e.g. S) bulkier than CH<sub>2</sub> within the part of the side chain of L-AcK between the  $\alpha$ -carbon and acetamide.

#### 4. Conclusion

In the current study, peptides containing L-AcK or its side chain modified analogs were prepared and assayed using human SIRT1. Our results suggested that SIRT1-catalyzed deacetylation reaction had a very stringent requirement for the distance between the  $\alpha$ -carbon and the side chain acetamido group, with that found in L-AcK being optimal. Moreover, our current study showed that SIRT1 catalyzed the stereospecific deacetylation of L-AcK versus its D-isomer. Taken together with the previous demonstration that the side chain acetyl group of L-AcK can be extended to bulkier acyl groups for Sir2-catalyzed lysine N<sup>ε</sup>-deacylation reaction, and the highly conserved nature of the Sir2 enzyme catalytic domain [1–3], the results from our current study shall constitute another piece of important information to be considered when designing inhibitors for SIRT1 and Sir2 enzymes in general.

#### Acknowledgments

The financial support from the James L. and Martha J. Focht Endowment, the University of Akron Research Foundation, and the University of Akron Faculty Research Fellowship is greatly appreciated. We thank Prof. Tony Kouzarides (University of Cambridge, UK) for the GST-SIRT1 plasmid. We also thank Prof. Chrys Wesdemiotis and his research group at the University of Akron for the assistance with mass spectrometric analysis of the compounds used in the current study. We wish to thank The Goodyear Corporation for donation of the NMR instrument (Varian Mercury 300) used in this work. We also wish to thank The National Science Foundation (CHE-8808587) for funds used to purchase the NMR instrument (Varian GEMINI 300) used in this work.

#### References

- [1] S. Thiagalingam, K.H. Cheng, H.J. Lee, N. Mineva, A. Thiagalingam, J.F. Ponte, *Ann. NY. Acad. Sci.* 983 (2003) 84–100.
- [2] I.V. Gregoret, Y.M. Lee, H.V. Goodson, *J. Mol. Biol.* 338 (2004) 17–31.
- [3] L.R. Saunders, E. Verdin, *Oncogene* 26 (2007) 5489–5504.
- [4] G. Blander, L. Guarente, *Annu. Rev. Biochem.* 73 (2004) 417–435.
- [5] J.M. Denu, *Curr. Opin. Chem. Biol.* 9 (2005) 431–440.
- [6] A.A. Sauve, C. Wolberger, V.L. Schramm, J.D. Boeke, *Annu. Rev. Biochem.* 75 (2006) 435–465.
- [7] S.C. Hodawadekar, R. Marmorstein, *Oncogene* 26 (2007) 5528–5540.
- [8] X.J. Yang, E. Seto, *Oncogene* 26 (2007) 5310–5318.
- [9] K. Batta, C. Das, S. Gadad, J. Shandilya, T.K. Kundu, *Subcell. Biochem.* 41 (2007) 193–212.
- [10] H. Yamamoto, K. Schoonjans, J. Auwerx, *Mol. Endocrinol.* 21 (2007) 1745–1755.
- [11] S. Michan, D. Sinclair, *Biochem. J.* 404 (2007) 1–13.
- [12] B. Schwer, E. Verdin, *Cell Metab.* 7 (2008) 104–112.

- [13] T. Finkel, C.X. Deng, R. Mostoslavsky, *Nature* 460 (2009) 587–591.
- [14] M. Porcu, A. Chiarugi, *Trends Pharmacol. Sci.* 26 (2005) 94–103.
- [15] L. Gan, *Drug News Perspect.* 20 (2007) 233–239.
- [16] P.J. Elliott, M. Jirousek, *Curr. Opin. Investig. Drugs* 9 (2008) 371–378.
- [17] T.F. Outeiro, O. Marques, A. Kazantsev, *Biochim. Biophys. Acta* 1782 (2008) 363–369.
- [18] W. Deppert, *Cell Cycle* 7 (2008) 2947–2948.
- [19] J.C. Milne, J.M. Denu, *Curr. Opin. Chem. Biol.* 12 (2008) 11–17.
- [20] A.A. Sauve, *Curr. Pharm. Des.* 15 (2009) 45–56.
- [21] S. Imai, W. Kiess, *Front. Biosci.* 14 (2009) 2983–2995.
- [22] T. Liu, P.Y. Liu, G.M. Marshall, *Cancer Res.* 69 (2009) 1702–1705.
- [23] R.C. Neugebauer, W. Sippl, M. Jung, *Curr. Pharm. Des.* 14 (2008) 562–573.
- [24] B.C. Smith, W.C. Hallows, J.M. Denu, *Chem. Biol.* 15 (2008) 1002–1013.
- [25] Z. Cheng, Y. Tang, Y. Chen, S. Kim, H. Liu, S.S. Li, W. Gu, Y. Zhao, *Mol. Cell. Proteom.* 8 (2009) 45–52.
- [26] B.C. Smith, J.M. Denu, *J. Biol. Chem.* 282 (2007) 37256–37265.
- [27] B.C. Smith, J.M. Denu, *J. Am. Chem. Soc.* 129 (2007) 5802–5803.
- [28] W.F. Hawse, K.G. Hoff, D.G. Fatkins, A. Daines, O.V. Zubkova, V.L. Schramm, W. Zheng, C. Wolberger, *Structure* 16 (2008) 1368–1377.
- [29] J. Garrity, J.G. Gardner, W. Hawse, C. Wolberger, J.C. Escalante-Semerena, *J. Biol. Chem.* 282 (2007) 30239–30245.
- [30] T. Asaba, T. Suzuki, R. Ueda, H. Tsumoto, H. Nakagawa, N. Miyata, *J. Am. Chem. Soc.* 131 (2009) 6989–6996.
- [31] D.A. Wellings, E. Atherton, *Methods Enzymol.* 289 (1997) 44–67.
- [32] E. Langley, M. Pearson, M. Faretta, U.M. Bauer, R.A. Frye, S. Minucci, P.G. Pelicci, T. Kouzarides, *EMBO J.* 21 (2002) 2383–2396.
- [33] A.J. Bannister, A. Cook, T. Kouzarides, *Oncogene* 6 (1991) 1243–1250.
- [34] B.J. North, B. Schwer, N. Ahuja, B. Marshall, E. Verdin, *Methods* 36 (2005) 338–345.
- [35] R. Lutgring, K. Sujatha, J. Chmielewski, *Bioorg. Med. Chem. Lett.* 3 (1993) 739–742.
- [36] Merck Biosciences, *Novabiochem® Guide to the selection of building blocks for peptide synthesis*, 2009.
- [37] H. Lamthanh, C. Roumestand, C. Deprun, A. Ménez, *Int. J. Pept. Protein Res.* 41 (1993) 85–95.
- [38] T. Soussi, P. May, *J. Mol. Biol.* 260 (1996) 623–637.
- [39] H. Vaziri, S.K. Dessain, E. Ng Eaton, S.I. Imai, R.A. Frye, T.K. Pandita, L. Guarente, R.A. Weinberg, *Cell* 107 (2001) 149–159.
- [40] A.L. Garske, J.M. Denu, *Biochemistry* 45 (2006) 94–101.
- [41] K.G. Hoff, J.L. Avalos, K. Sens, C. Wolberger, *Structure* 14 (2006) 1231–1240.
- [42] J.L. Avalos, I. Celic, S. Muhammad, M.S. Cosgrove, J.D. Boeke, C. Wolberger, *Mol. Cell* 10 (2002) 523–535.
- [43] D.G. Fatkins, A.D. Monnot, W. Zheng, *Bioorg. Med. Chem. Lett.* 16 (2006) 3651–3656.
- [44] D.G. Fatkins, W. Zheng, *Int. J. Mol. Sci.* 9 (2008) 1–11.
- [45] N. Jamonnak, D.G. Fatkins, L. Wei, W. Zheng, *Org. Biomol. Chem.* 5 (2007) 892–896.
- [46] B.C. Smith, J.M. Denu, *Biochemistry* 46 (2007) 14478–14486.